Trans. Phenom. Nano Micro Scales, 3(2): 106-117, Summer – Autumn 2015
DOI: 10.7508/tpnms.2015.02.005

ORIGINAL RESEARCH PAPER

Turbulent Mixed Convection of a Nanofluid in a Horizontal Circular Tube with Non-Uniform Wall Heat Flux Using a Two-Phase Approach

F. Vahidinia[1,*], M. Rahmdel[2]
[1]*Mechanical Engineering Department, University of Zabol, Zabol, I.R. Iran*
[2] *Mechanical Engineering Department, University of Sistan and Baluchestan, Zahedan, I.R.Iran*

ARTICLE INFO.

Article history
Received 14 November 2014
Accepted 23 May 2015

Keywords
Grashof number
Horizontal tube
Mixed convection
Nanoparticles volume fraction
Turbulent flow

Abstract

In this paper, Turbulent mixed convective heat transfer of water and Al_2O_3 nanofluid has been numerically studied in a horizontal tube under non-uniform heat flux on the upper wall and insulation in the lower wall using mixture model. For the discretization of governing equations, the second-order upstream difference scheme and finite volume method were used. The coupling of pressure and velocity was established by using SIMPLEC algorithm. The calculated results demonstrated that the convective heat transfer coefficient of nanofluid is higher than of the base fluid and by increasing the nanoparticles volume fraction, the convective heat transfer coefficient and shear stress on the wall increase. On the other hand, with increasing the Grashof number, the shear stress and convective heat transfer coefficient decrease.

1. Introduction

In the field of heat transfer, the main concern of the researchers was improving the thermal performance of the heat exchanger systems**.** For this purpose, various methods have been employed to enhance the heat transfer. These methods include passive and active procedures [1-8]. But the other way that extensive studies have been conducted in this field, is adding metal and nonmetal particles to the base fluid in the nanoscale size. Research studies have often focused on the particles such as Cu, Al_2O_3, TiO_2, SiO2, Fe_3O_4 and the base fluid such as water, ethylene glycol (EG), kerosene, and engine oil.

In these studies, various methods of convective heat transfer have been investigated both numerically and experimentally with different boundary conditions and cross sections which include forced convection, mixed convection, and natural convection. The nanofluid flow considered laminar or turbulent in tubes with different angles, horizontal, vertical, and inclined. In these investigations, nanoparticles with different volume fractions (usually 0-0.06) and various diameters (often 0-100nm) were considered and their effects on the parameters such as Nusselt number, convective heat transfer coefficient, wall shear stress, and surface friction coefficient were investigated for different thermo-fluid conditions. Most of these scientists believed that the suspension of nanoparticles in the base fluid improves the efficiency of thermal systems [9-21].

[*]Corresponding author
Email address: f.vahidinia@gmail.com

Nomenclature

C_f	average skin friction coefficient
Cp	specific heat of the fluid (J/kg K)
df	molecular diameter of base fluid (nm)
dp	nanoparticle diameter (nm)
D	tube diameter (m)
G	generation Turbulence kinetic energy
g	gravity acceleration (m/s^2)
Gr	Grashof number ($Gr = \frac{g\beta_{eff} q_w D^4}{\lambda_{eff} \nu_{eff}^2}$)
h	average convective heat transfer coefficient
k	turbulent kinetic energy (m^2/s^2)
L	channel length (m)
P	pressure (Pa)
q	Average wall heat flux (W/m^2)
r	radial coordinate (m)
Re	Reynolds number ($Re = \frac{\rho VD}{\mu}$)
T,t	time averaged and fluctuating temperature
V,v	time averaged and fluctuating velocity
z	axial coordinate (m)

Greek Symbols

α	Thermal diffusivity
β	Volumetric expansion coefficient (K^{-1})
ε	dissipation of turbulent kinetic energy (m^2/s)
θ	Angular coordinate
ϕ	particle volume fraction
λ	thermal conductivity of the fluid (W/mK)
μ	fluid dynamic viscosity (Kg /m.s)
ρ	fluid density (Kg/m^3)
τ	shear stress (Pa)

Subscripts

b	bulk value
f	primary phase
k	k-th phase
m	mixture
p	particle, secondary phase
s	solid
t	turbulent
w	wall
i	inner condition

The effect of water-based Al_2O_3 nanofluid and water-based Al_2O_3-Cu hybrid nanofluid on the laminar forced convective heat transfer in a horizontal circular tube investigated numerically by Moghadassi et al. [22]. They concluded that the average Nusselt number of nanofluid is higher than of the base fluid. Also, the convective heat transfer coefficient for the hybrid nanofluid is higher than of water-based Al_2O_3 nanofluid. Wusiman et al. [23] experimentally investigated the forced convective heat transfer in both laminar and turbulent flow. Bianco et al. [24] carried out a numerical investigation on the turbulent flow forced convection of water–Al_2O_3 nanofluid in a circular tube. They used both single-phase and two-phase models and found that the two-phase mixture model is better than the single-phase model. As they showed, with increasing the particle's volume fraction, convective heat transfer coefficient increases. Saha and Paul [25] numerically analyzed the turbulent mixed convective heat transfer of the Al_2O_3–water and TiO_2–water nanofluids flowing through a horizontal circular tube using the two-phase mixture model.

It is shown that TiO_2–water nanofluid is the most energy efficient coolant than Al_2O_3–water nanofluid. Aghaei et al. [26] investigated numerically the turbulent forced convective heat transfer behavior of alumina nanoparticle dispersions in water in a horizontal tube.

They found that by increasing the Reynolds number, the surface friction coefficient decreases and the pressure drop increases with the increase of volume fractions and Reynolds number.

In this paper, turbulent mixed convective heat transfer of water and Al_2O_3 nanofluid is numerically studied in a horizontal tube under non-uniform heat flux on the upper wall and insulation in the lower wall using two phase mixture model**.** The effects of nanoparticles volume fraction on the hydrodynamic and thermal parameters are presented and discussed for different Grashof number.

2. Mathematical modeling

Turbulent mixed convective of water and Al_2O_3 nanofluid in a horizontal circular tube with non-uniform heat flux on the upper wall and insulation in the lower wall is considered. In order to discretize the governing equations, the second-order upstream

difference scheme and finite volume method are used. Figure 1 shows the considered geometrical configuration. The tube has a diameter of 0.01m and a length of 1m. The tube thickness to diameter ratio of 0.1 is assumed.

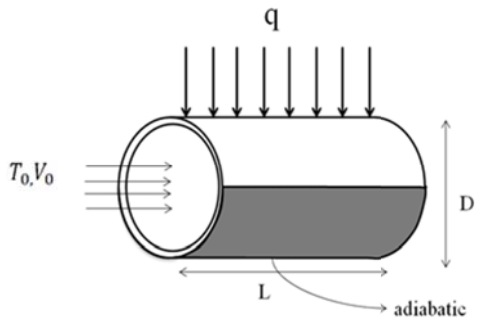

Fig. 1. Schematic of the considered horizontal tube

In this paper, the two phase mixture model is employed for the simulation. Behzadmehr et al. [27] used two-phase mixture model for the first time. They showed that the two phase mixture model is more precise than the single phase approach. Different authors also compared single phase model and mixture model and showed that the mixture model is in a better agreement with the experimental results [28]. Some researchers also compared the two-phase Eulerian models and mixture model and concluded that the mixture model is in a better agreement with the experimental results for the estimation of average Nusselt number [29]. According to the literature the two-phase mixture model is more suitable for the solution of nanofluid flow in a tube [30-37], so the two-phase mixture model is implemented in this study. The thermos-physical properties of the nanofluid are assumed constant except for the density in the momentum equation, which varies linearly with the temperature (Boussinesq's hypothesis).

The conservation equations for steady state incompressible flow using mixture model are as follows [33]:

Continuity equation:

$$\nabla.(\rho_m V_m) = 0 \tag{1}$$

Conservation of momentum:

$$\nabla.\left(\rho_m V_m V_m\right) = -\nabla p_m + \nabla.\left[\tau - \tau_t\right] - \rho_{eff}\beta_{eff}(T - T_o)g + \nabla.\left(\sum_{k=1}^{n} \phi_k \rho_k V_{dr,k} V_{dr,k}\right) \tag{2}$$

Conservation of energy:

$$\nabla.(\phi_k V_k (\rho_k h_k + p)) = \nabla.(\lambda_{eff} \nabla T - C_p \rho_m \overline{vt}) \tag{4}$$

where V_m, ρ_m and μ_m are the mass-average velocity of the mixture, mixture density and viscosity of the mixture respectively and defined as

$$V_m = \frac{\sum_{k=1}^{n} \phi_k \rho_k V_k}{\rho_{eff}}, \quad \rho_m = \sum_{k=1}^{n} \phi_k \mu_k, \quad \mu_m = \sum_{k=1}^{n} \phi_k \mu_k \tag{5}$$

In equation 2, $V_{dr,k}$ is the drift velocity for the secondary phase k, i.e. the nanoparticles in the present study which is defined as

$$V_{dr,k} = V_k - V_m \tag{6}$$

And in equation 2, τ and τ_t are the viscous shear stress and turbulent shear stress, respectively which are defined as:

$$\tau = \mu_m \nabla V_m, \quad \tau_t = -\sum_{k=1}^{n} \phi_k \rho_k \overline{v_k v_k} \tag{7}$$

In the above equation, μ_m and v_k are the viscosity of the nanofluid and the fluctuating velocity phase k.

V_{pf} is the slip velocity or relative velocity that defines as the velocity of a secondary phase (p) relative to the velocity of the primary phase (f).

$$V_{pf} = V_p - V_f \tag{8}$$

The drift velocity is related to the relative velocity which is defined as:

$$V_{dr,k} = V_{pf} - \sum_{k=1}^{n} \frac{\phi_k \rho_k}{\rho_m} V_{fk} \tag{9}$$

The relative velocity is determined from equation 8 proposed by Manninen et al. [38]

$$V_{pf} = \frac{\rho_p d_p^2}{18\mu_f f_{drag}} \frac{\left(\rho_p - \rho_m\right)}{\rho_p} \boldsymbol{a} \tag{10}$$

In this equation the drag function, f_{drag} is calculated by Schiller and Naumann [39]

$$f_{drag} = \begin{cases} 1+0.15Re_p^{0.687}, & Re_p \le 1000 \\ 0.0183Re_p, & Re_p \ge 1000 \end{cases} \quad (11)$$

The acceleration (a) in equation 10 is:

$$\boldsymbol{a} = \boldsymbol{g} - (V_m.\nabla)V_m \quad (12)$$

3. Turbulence modeling

Turbulence is modeled with the Launder and Spalding [40] k–ε turbulence model for the mixture. It is expressed by equations 13-15:

$$\nabla.(\rho_m V_m k) = \nabla.(\frac{\mu_{t,m}}{\sigma_k}\nabla k) + G_{k,m} - \rho_m \varepsilon \quad (13)$$

$$\nabla.(\rho_m V_m \varepsilon) = \nabla.(\frac{\mu_{t,m}}{\sigma_\varepsilon}\nabla k) + \frac{\varepsilon}{k}(c_1 G_{k,m} - c_2 \rho_m \varepsilon) \quad (14)$$

$$\mu_{t,m} = \rho_m c_\mu \frac{k^2}{\varepsilon}$$
$$G_{k,m} = \mu_{t,m}(\nabla V_m + (\nabla V_m)^T) \quad (15)$$

$$c_1 = 1.44, c_2 = 1.92, c_\mu = .09, \sigma_k = 1, \sigma_\varepsilon = 1.3$$

4. Boundary conditions

The boundary conditions are expressed as follows:
•At inlet of tube (Z = 0):

$$V_z = V_0 \quad , V_\theta = V_r = 0 \quad , T = T_0 \quad , I = I_0 \quad (16)$$

Turbulent intensity calculates based on the formula [41]:

$$I_0 = 0.16(Re)^{-1/8} \quad (17)$$

• At the tube wall ($r=r_0$):

$$0 \le \theta \le \pi : \quad -k_s \frac{\partial T_s}{\partial r} = q_w \quad (18)$$

$$\pi \le \theta \le 2\pi : \; -k_s \frac{\partial T_s}{\partial r} = 0 \quad (19)$$

• At the solid/fluid inter face: ($r = r_i$):

$$T_w = T_{nf} \;,\; k_s \frac{\partial T_w}{\partial r} = k_{eff} \frac{\partial T_{nf}}{\partial r}$$
$$V_z = V_r = V_\theta = 0 \quad (20)$$

•At the tube outlet:
The diffusion fluxes are set to zero at the exit for all dependent variables and an overall mass balance correction is obeyed.

5. Nanofluids thermo-physical properties

The physical properties are:
Effective density:
The nanofluid density is given by [42]:

$$\rho_m = (1-\phi)\rho_f + \phi\rho_p \quad (21)$$

Where the volumetric concentration is given by [43].

$$\phi = \frac{\rho_f \phi_m}{\rho_f \phi_m + \rho_p (1-\phi_m)} \quad (22)$$

Where Φ_m is the mass fraction.

An accurate equation is used for calculating the effective heat capacitance [44].

$$(C_p)_{eff} = \left[(1-\phi)(\rho C_p)_f + \phi(\rho C_p)_p\right] \Big/ \rho_m \quad (23)$$

The thermal conductivity of the nanofluid is calculated from Chon et al. [45] correlation, which considers the Brownian motion and mean diameter of the nanoparticles.

$$k_{eff}/k_f = 1 + 64.7 \times \phi^{0.746} (d_f/d_p)^{0.369} (k_p/k_f)^{0.746} \times pr^{.9955} \times R\,e^{1.2321} \quad (24)$$

Where Pr and Re in equation 24 are defined as:

$$pr = \frac{\mu_f}{\rho_f \alpha_f} \quad , \quad Re = \frac{\rho_f B_c T}{3\pi\mu^2 l_{bf}}$$
$$\mu = A \times 10^{\frac{B}{T-C}}, C = 140, B = 247, A = 2.414e-5 \tag{25}$$

l_{bf} is the mean free path of water and B_c is the Boltzman constant ($B_c = 1.3807 \times 10^{-23}$ J/K).

Effective viscosity is calculated by the following equation proposed by Masoumi et al. [46] that considers the effects of volume fraction, density, and average diameter of nanoparticles and physical properties of the base fluid:

$$\mu_{eff} = \mu_f + \frac{\rho_P V_B d_P^2}{72C\delta}, \quad V_B = \frac{1}{d_P}\sqrt{\frac{18K_b T}{\pi\rho_P d_P}}$$
$$, \quad \delta = \sqrt[3]{\frac{\pi}{6\phi}} d_P \tag{26}$$

$$C = \mu_f^{-1}\left[\left(c_1 d_p + c_2\right)\phi + \left(c_3 d_p + c_4\right)\right] \tag{27}$$

Where C_1, C_2, C_3 and C_4 are:

$C_1 = -0.000001133, \quad C_2 = -0.000002721$

$C_3 = -0.00000009, \quad C_4 = -0.000000393$

Thermal expansion coefficient proposed by Khanafer et al. [47]:

$$\beta_{eff} = \begin{bmatrix} \beta_p / \left(1 + (1-\phi)\rho_f / \phi\rho_p\right)\beta_f + \\ 1 / \left(1 + \phi\rho_p / (1-\phi)\rho_f\right) \end{bmatrix} \tag{28}$$

6. Numerical method and validation

In this study, the fluid enters the tube with a constant inlet temperature T_{in} of 293 K and with uniform axial velocity of V_{in}. This set of coupled nonlinear differential equations is discretized by using the control volume method.

The second order upstream method is used for the convective and diffusive terms and SIMPLEC procedure is adopted for the velocity–pressure coupling.

The computation is discretized by using a structured non-uniform grid distribution. It is finer near the tube entrance and near the wall where the velocity and temperature gradients are significant.

Several different grid distributions are selected and tested to ensure that the calculated results are grid independent.

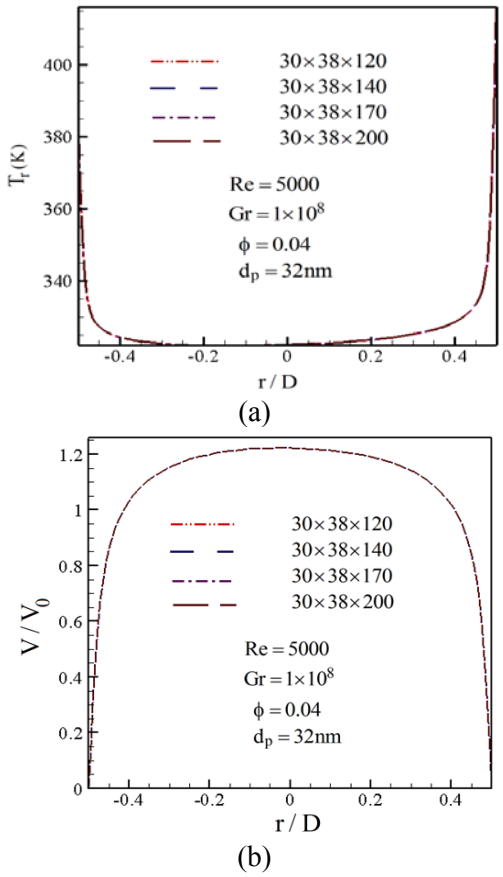

Fig. 2. Grid independence test: (a) fully developed temperature (b) centerline axial velocity

It is consisted of 170, 30, and 38 nodes, respectively, in the axial, radial, and circumferential directions.

As shown in figure 2, increasing the grid numbers do not significantly change the velocity and temperature of the nanofluid. Different axial and radial profiles are also tested to be sure that the results are grid independent. To show the validity and also precision of the model and numerical procedure, comparisons with the available experimental and numerical simulation are done. As it is shown in figures 3 a-b, good agreements between the results are observed.

with increasing the volume fraction of nanoparticles, the heat flux on the wall is increased and therefore, buoyancy forces increase. On the other hand, in a constant Reynolds number, with increasing the

volume fraction of nanoparticles, the flow velocity is increased and therefore, inertial forces increase.

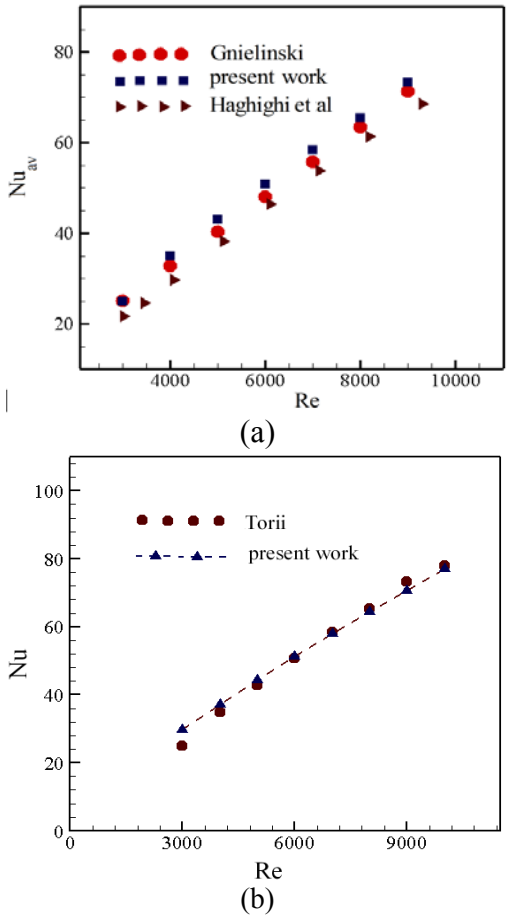

Fig. 3. a) Comparison of the axial evolution of Nu in a horizontal tube with the results obtained by Gnielinski [48] and Haghighi et al [49], b) Comparison of the axial evolution of Nu in a horizontal tube with the experimental results obtained by S. Torii [50].

Figure 3a shows the comparison between calculated results and the results obtained by Gnielinski [48] and experimental results obtained by Haghighi et al. [49].Another comparison is also performed with the experimental results obtained by Torii [50] (see figure 3b).

7. Results and Discussions

Numerical investigations were carried out using Al_2O_3-water nanofluid, Reynolds number of Re= 5×10^3 different Grashof numbers (Gr = 25×10^6, Gr = 1×10^8) and different nano particle concentrations (0%, 2%, 4% and 5%). Figure 4 show the dimensionless axial velocity profiles for different nanoparticles volume fraction at the fully developed region of Z/D=94. It is found that with increasing the nanoparticles volume fraction, axial velocity profiles become more uniform.

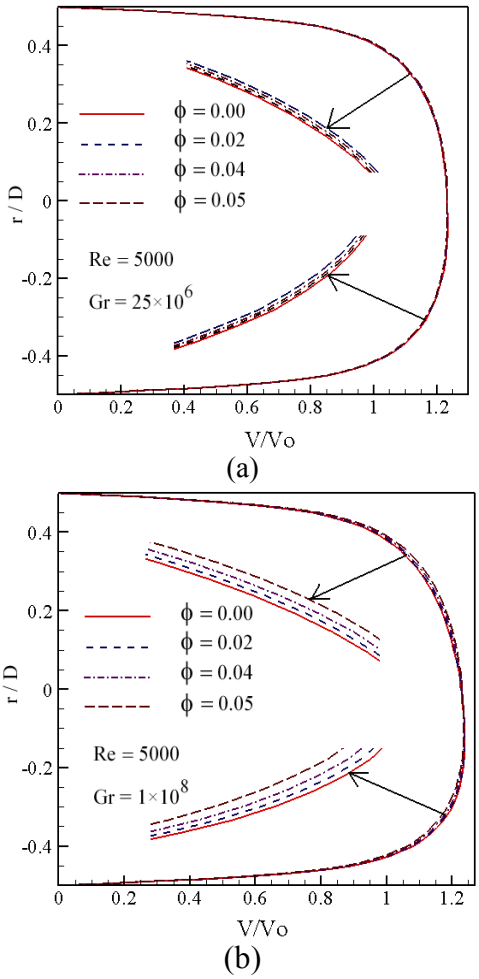

Fig. 4. Variation of the dimensionless fully developed axial velocity profiles with different Grashof number for Al_2O_3–water nanofluid, nanoparticle volume concentration of 0, 0.02, 0.04 and 0.05 and Reynolds number of 5000.

As it is clearly seen, increasing the Grashof number augments the buoyancy forces and therefore, the maximum axial velocity approaches to the near wall region at the upper part of the tube.

Figure 5 shows the turbulent kinetic energy profile at the fully developed region of Z/D=94 at different particles volume fractions.

It can be seen that the turbulent kinetic energy increases with increasing the volume fraction of particles. This is due to the disturbances with increasing volume fraction. On the other hand, it is shown that with increasing Grashof number (Gr =

25×106 to Gr = 1×108), the dimensionless turbulent kinetic energy profiles tend to the lower wall, because the buoyancy forces are increased by increasing the Grashof number.

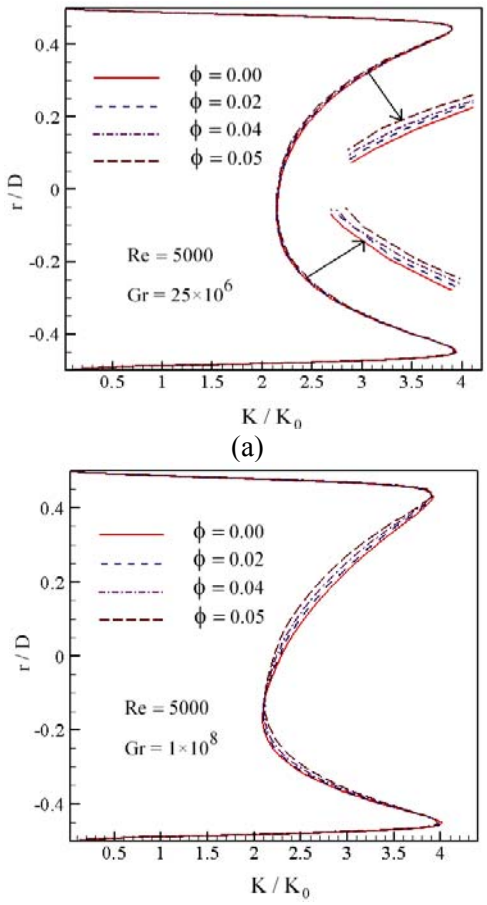

Fig. 5. Variation of the dimensionless fully developed turbulent kinetic energy profiles with different Grashof number for Al_2O_3–water nanofluid, nanoparticle volume concentration of 0, 0.02, 0.04 and 0.05 and Reynolds number of 5000.

For a given Reynolds number and different nanoparticles volume fraction (0, 2, 4 and 5%), vectors of secondary flow at the fully developed region of Z/D=94 are presented in Figure 6a for Gr = 25×10^6 . Considering the constant Grashof number, By Superposition of these two factors, the secondary flow does not change significantly.

In figure 6b, the vectors of secondary flow are shown for Gr = 1×10^8.

By comparing figure 6 a-b it can be seen, by increasing the Grashof number, the vectors of secondary flow do not change. The reason of this issue is the balance of the buoyancy forces with increasing Grashof number. This means that nanoparticles volume fraction and Grashof number do not have significant effect on the secondary flow in the present study.

Figure 7 shows the dimensionless temperature profiles for different nanoparticles volume fraction at the fully developed region of Z/D=94. It can be seen that the dimensionless temperature decreases with increasing the volume fraction of nanoparticles. By increasing the nanoparticles volume fraction, heat flux on the wall and the thermal conductivity increase; therefore, the dimensionless temperature decreases. On the other hand, with increasing the Grashof number, the dimensionless temperature decreases. The reason is that, the heat flux on the wall increases.

Figure 8 shows the effect of nanoparticles volume fraction on the shear stress changes along the tube length for a given Reynolds number (Re=5000) at two different Grashof numbers (Gr = 25×10^6 and Gr = 1×10^8). As can be seen, the shear stress decreases at the tube entrance and then remains constant. With increasing volume fraction of nanoparticles, thermo-physical characteristics of nanofluids are changed. One of these characteristics in the turbulent flow is the viscosity of nanofluid. By increasing the volume fraction of the nanoparticles, viscosity of nanofluid is increased.

In a constant Reynolds number, with increase of viscosity, the velocity of nanofluid and the velocity gradient are increased. Therefore, with increasing these factors, the shear stress of nanofluid is increased in the turbulent flow. On the other side, by increasing the Grashof number, the shear stress on the wall decreases. The reason is that, the velocity of nanofluid and the velocity gradient are decreased by increasing the Grashof number.

Figure 9 shows the effect of nanoparticles volume fraction on the convective heat transfer coefficient along the tube length for a given Reynolds number at two different Grashof numbers. It can be seen that convective heat transfer coefficient is too high at the beginning of the tube next to the tube inlet because of the proximity of the wall temperature and the bulk fluid temperatures.

Then, it remains constant in the developed region due to the same temperature difference.

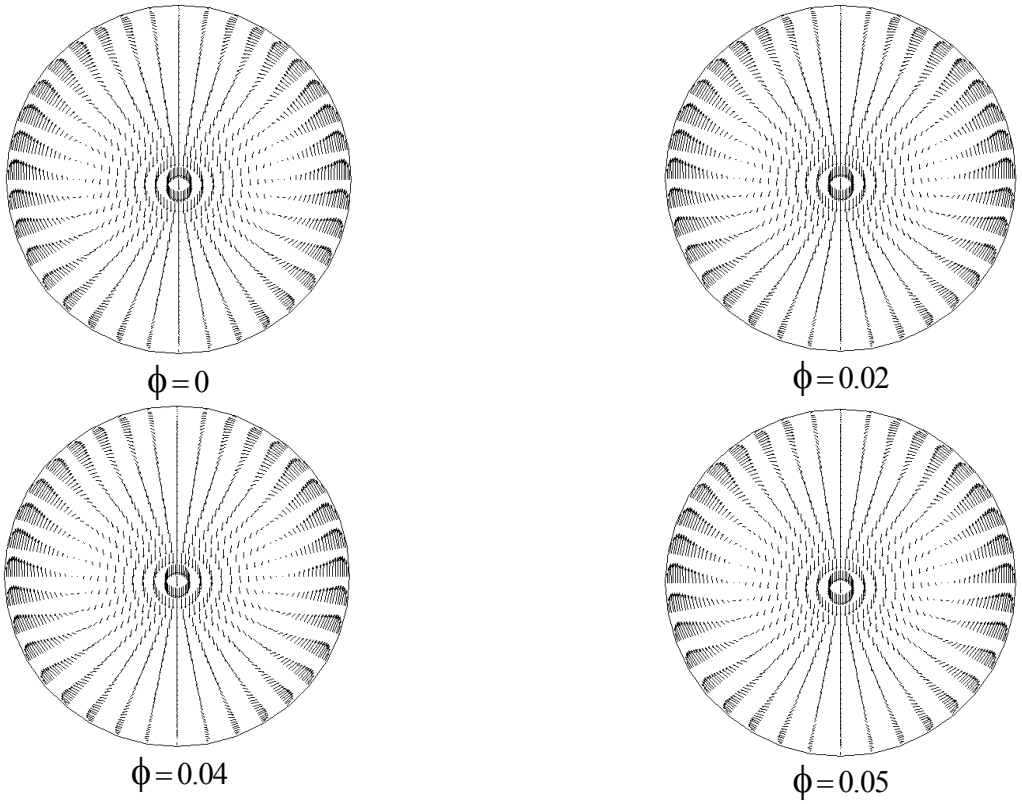

Fig.6a. Effect of nanoparticles concentration on the Vectors of secondary flow for different volume fraction at Gr = 25×10^6

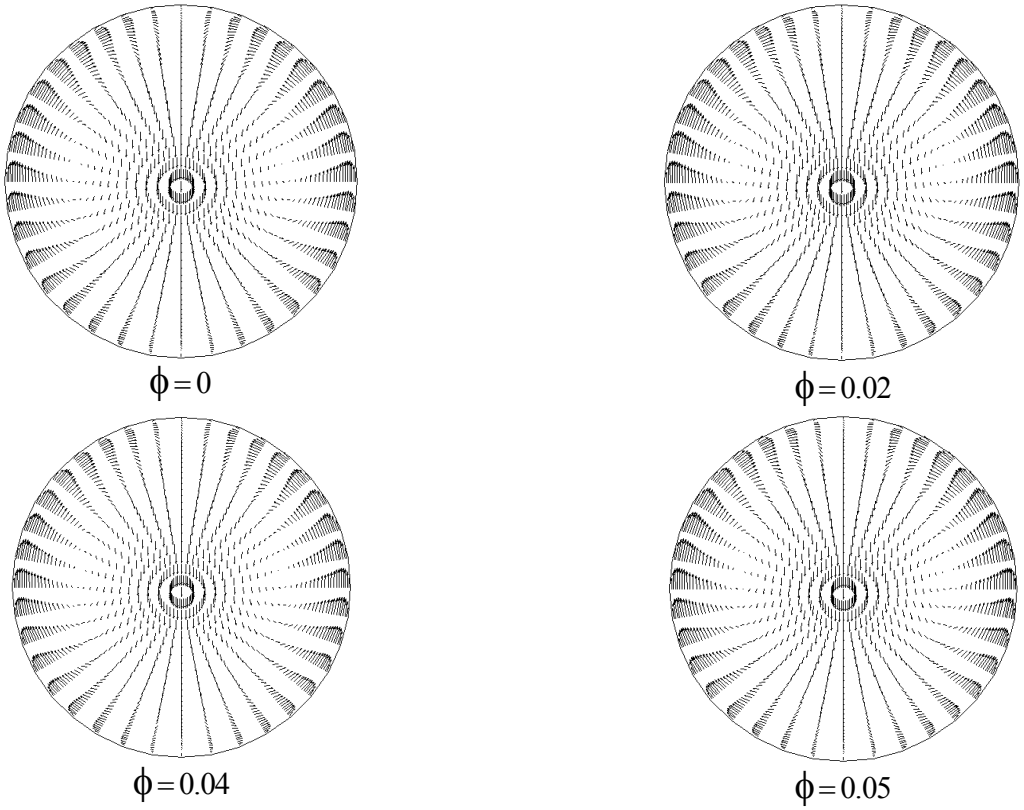

Fig.6b. Effect of nanoparticles concentration on the Vectors of secondary flow for different volume fraction at Gr = 1×10^8

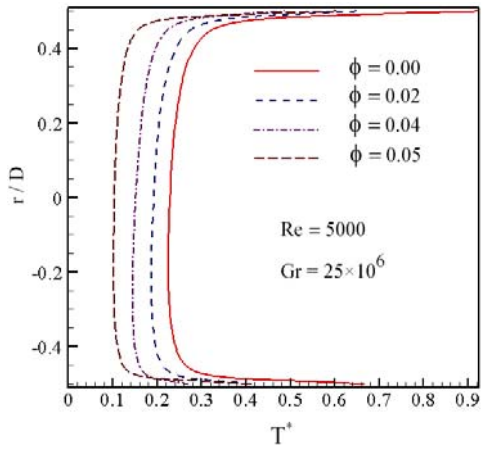

(a)

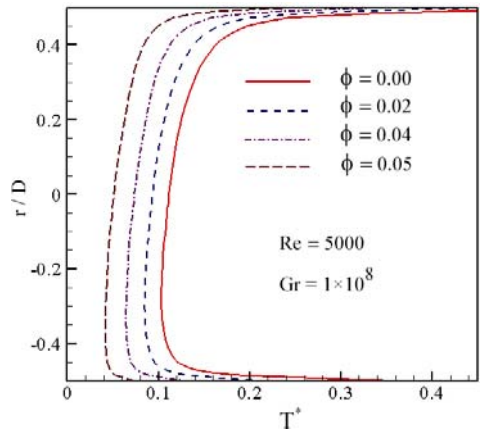

(b)

Fig. 7. Variation of the dimensionless fully developed temperature profiles with different Grashof number for Al_2O_3–water nanofluid, nanoparticle volume concentration of 0, 0.02, 0.04 and 0.05 and Reynolds number of 5000.

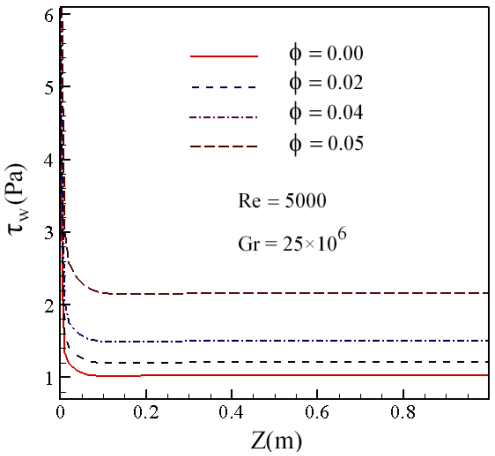

(a)

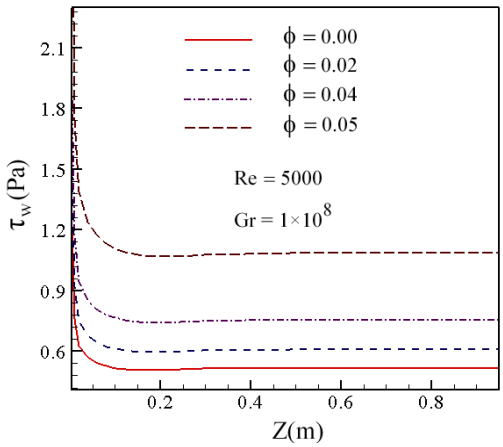

(b)

Fig. 8. Variation of the shear stress along the tube length with different Grashof number for Al_2O_3–water nanofluid, nanoparticle volume concentration of 0, 0.02, 0.04 and 0.05 and Reynolds number of 5000.

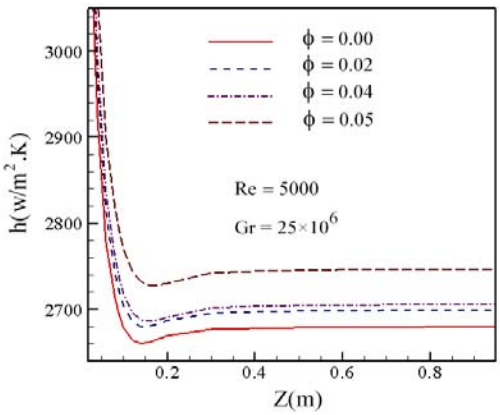

(a)

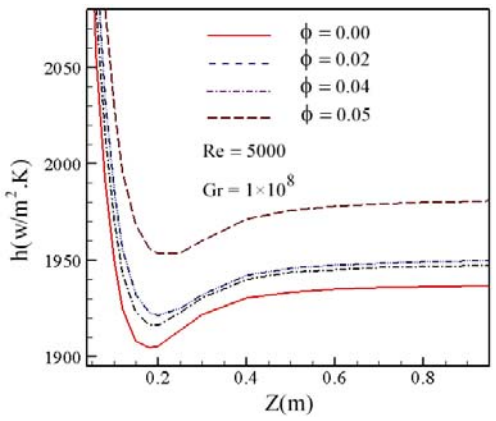

(b)

Fig.9. Variation of the convective heat transfer coefficient along the tube length with different Grashof number for Al_2O_3–water nanofluid, nanoparticle volume concentration of 0, 0.02, 0.04 and 0.05 and Reynolds number of 5000.

In all cases, the convective heat transfer coefficient decreases at the tube entrance, then remains constant. The convective heat transfer coefficient increases with increasing the nanoparticles volume fraction. The main reason for this is that by increasing the volume fraction, the physical properties of nanofluids are improved. Another reason of enhancing the convective heat transfer coefficient of nanofluid in the turbulent flow is the increase of disturbances of flow with increasing volume fraction nanoparticles. On the other side, by increasing the Grashof number, the convective heat transfer coefficient decreases. The reason is that, the velocity and the disturbances of flow are decreased with the increase of Grashof number.

8. Conclusion

Numerical investigations were carried out on the turbulent mixed convection heat transfer of the Al_2O_3–water nanofluids in a horizontal circular tube using the two-phase mixture model. The upper wall is under non-uniform heat flux and the lower wall is insulated. The results show that increasing the volume fraction of nanoparticles and Grashof number do not effect significantly on the secondary flow. By increasing the volume fraction of nanoparticles, the convective heat transfer coefficient and the shear stress on the wall are increased and the dimensionless temperature decreases. On the other hand, with increasing the Grashof number, the convective heat transfer coefficient, the shear stress on the wall and the dimensionless temperature are decreased.

References

[1] P.W. Deshmukh, R.P. Vedula, Heat transfer and friction factor characteristics of turbulent flow through a circular tube fitted with vortex generator inserts, International Journal of Heat and Mass Transfer 79 (2014) 551–560.

[2] T. Wenbin, T. Yong, Z. Bo, L. Longsheng, Experimental studies on heat transfer and friction factor characteristics of turbulent flow through a circular tube with small pipe inserts, International Communications in Heat and Mass Transfer 56 (2014) 1–7.

[3] A.F. Wibisono, Y. Addad, J.I. Lee, Numerical investigation on water deteriorated turbulent heat transfer regime in vertical upward heated flow in circular tube, International Journal of Heat and Mass Transfer 83 (2015) 173–186.

[4] J. Wen, H. Yang, S. Wang, S. Xu, Y. Xue, H. Tuo, Numerical investigation on baffle configuration improvement of the heat exchanger with helical baffles, Energy Conversion and Management 89 (2015) 438–448.

[5] J. Zhang, Y. Zhao, Y. Diao, Y. Zhang, An experimental study on fluid flow and heat transfer in a multiport minichannel flat tube with micro-fin structures, International Journal of Heat and Mass Transfer 84 (2015) 511–520.

[6] S.P. Guo, Z. Wu, W. Li, D. Kukulka, B. Sunden, X.P. Zhou, J.J. Wei, T. Simon, Condensation and evaporation heat transfer characteristics in horizontal smooth, herringbone and enhanced surface EHT tubes, International Journal of Heat and Mass Transfer 85 (2015) 281–291.

[7] D.J. Kukulka, R. Smith, K.G. Fuller, Development and evaluation of enhanced heat transfer tubes, Applied Thermal Engineering 31 (2011) 2141–2145.

[8] C. Muthusamy, M. Vivar, I. Skryabin, K. Srithar, Effect of conical cut-out turbulators with internal fins in a circular tube on heat transfer and friction factor, International Communications in Heat and Mass Transfer 44 (2013) 64–68.

[9] R. Raj, N.S. Lakshman, Y. Mukkamala, Single phase flow heat transfer and pressure drop measurements in doubly enhanced tubes, International Journal of Thermal Sciences 88 (2015) 215-227.

[10] W.H. Azmi, K.V. Sharma, P.K. Sarma, R. Mamat, S. Anuar, L.S. Sundar, Numerical validation of experimental heat transfer coefficient with SiO_2 nanofluid flowing in a tube with twisted tape inserts, Applied Thermal Engineering 73 (2014) 296-306.

[11] T. Sokhansefat, A.B. Kasaeian, F. Kowsary, Heat transfer enhancement in parabolic trough collector tube using Al_2O_3/synthetic oil nanofluid, Renewable and Sustainable Energy Reviews 33 (2014) 636–644.

[12] K. Hadad, A. Rahimian, M.R. Nematollahi, Numerical study of single and two-phase models of water/Al_2O_3 nanofluid turbulent forced convection flow in VVER-1000 nuclear

reactor, Annals of Nuclear Energy 60 (2013) 287–294.

[13] M. Shariat, R. Mokhtari Moghari, A. Akbarinia, R. Rafee, S.M. Sajjadi, Impact of nanoparticle mean diameter and the buoyancy force on laminar mixed convection nanofluid flow in an elliptic duct employing two phase mixture model, International Communications in Heat and Mass Transfer 50 (2014) 15–24.

[14] A.A. Rabienataj Darzi, M. Farhadi, K. Sedighi, Heat transfer and flow characteristics of Al_2O_3–water nanofluid in a double tube heat exchanger, International Communications in Heat and Mass Transfer 47 (2013) 105–112.

[15] R.S. Vajjha, D.K. Das, D.R. Ray, Development of new correlations for the Nusselt number and the friction factor under turbulent flow of nanofluids in flat tubes, International Journal of Heat and Mass Transfer 80 (2015) 353–367.

[16] A. Malvandi, M.R. Safaei, M.H. Kaffash, D.D. Ganji, MHD mixed convection in a vertical annulus filled with Al_2O_3–water nanofluid considering nanoparticle migration, Journal of Magnetism and Magnetic Materials 382 (2015) 296–306.

[17] B.H. Salman, H.A. Mohammed, A.S. Kherbeet, Numerical and experimental investigation of heat transfer enhancement in a microtube using nanofluids, International Communications in Heat and Mass Transfer 59 (2014) 88–100.

[18] W.I.A. Aly, Numerical study on turbulent heat transfer and pressure drop of nanofluid in coiled tube-in-tube heat exchangers, Energy Conversion and Management 79 (2014) 304–316.

[19] S. Parvin, R. Nasrin, M.A. Alim, N.F. Hossain, A.J. Chamkha, Thermal conductivity variation on natural convection flow of water–alumina nanofluid in an annulus, International Journal of Heat and Mass Transfer 55 (2012) 5268–5274.

[20] Y. Abbassi, M. Talebi, A.S. Shirani, J. Khorsandi, Experimental investigation of TiO2/Water nanofluid effects on heat transfer characteristics of a vertical annulus with non-uniform heat flux in non-radiation environment, Annals of Nuclear Energy 69 (2014) 7–13.

[21] G. Dang, F. Zhong, Y. Zhang, X. Zhang, Numerical study of heat transfer deterioration of turbulent supercritical kerosene flow in heated circular tube, International Journal of Heat and Mass Transfer 85 (2015) 1003–1011.

[22] A. Moghadassi, E. Ghomi, F. Parvizian, A numerical study of water based Al_2O_3 and Al_2O_3−Cu hybrid nanofluid effect on forced convective heat transfer, International Journal of Thermal Sciences 92 (2015) 50-57.

[23] K. Wusiman, H. Chung, M.J. Nine, H. Afrianto, Heat transfer characteristics of nanofluid through circular tube, J. Cent. South Univ 20 (2013) 142−148.

[24] V. Bianco, O. Manca, S. Nardini, Performance analysis of turbulent convection heat transfer of Al_2O_3 water-nanofluid in circular tubes at constant wall temperature, Energy 77 (2014) 403-413.

[25] G. Saha, M.C. Paul, Heat transfer and entropy generation of turbulent forced convection flow of nanofluids in a heated pipe, International Communications in Heat and Mass Transfer 61 (2015) 26–36.

[26] A. Aghaei, G A. Sheikhzadeh, M. Dastmalchi, H. Forozande, Numerical investigation of turbulent forced-convective heat transfer of Al_2O_3–water nanofluid with variable properties in tube, Ain Shams Engineering Journal 6 (2015) 577-585.

[27] A. Behzadmehr, M. Saffar-Avval, N. Galanis, Prediction of Turbulent Forced Convection of a Nanofluid in a Tube with Uniform Heat Flux Using a Two Phase Approach, International Journal of Heat and Fluid Flow 28 (2007) 211–219.

[28] M. Hejazian, M. Keshavarz Moraveji , A. Beheshti, Comparative study of Euler and mixture models for turbulent flow of Al_2O_3 nanofluid inside a horizontal tube, International Communications in Heat and Mass Transfer 52 (2014) 152–158.

[29] V. Bianco, O. Manca, S. Nardini, Numerical investigation on nanofluids turbulent convection heat transfer inside a circular tube, International Journal of Thermal Sciences 50 (2011) 341–349.

[30] M. Akbari, A. Behzadmehr, F. Shahraki, Fully developed mixed convection in horizontal and inclined tubes with uniform heat flux using nanofluid, International Journal of Heat and Fluid Flow 29 (2008) 545–556.

[31] S. Mirmasoumi, A. Behzadmehr, Effect of nanoparticles mean diameter on mixed convection heat transfer of a nanofluid in a horizontal tube, International Journal of Heat

and Fluid Flow 29 (2008) 557–566.

[32] A. Akbarinia, A. Behzadmehr, Numerical study of laminar mixed convection of a nanofluidin horizontal curved tubes, Applied Thermal Engineering 27 (2007) 1327–1337.

[33] O. Ghaffari, A. Behzadmehr, H. Ajam, Turbulent mixed convection of a nanofluid in a horizontal curved tube using a two-phase approach, International Communications in Heat and Mass Transfer 37 (2010) 1551–1558.

[34] R. Mokhtari Moghari, A.S. Mujumdar, M. Shariat, F. Talebi, S.M. Sajjadi, A. Akbarinia, Investigation effect of nanoparticle mean diameter on mixed convection Al_2O_3-water nanofluid flow in an annulus by two phase mixture model, International Communications in Heat and Mass Transfer 49 (2013) 25–35.

[35] H. Aminfar, M. Mohammadpourfard, Y. NarmaniKahnamouei, A 3D numerical simulation of mixed convection of a magnetic nanofluid in the presence of non-uniform magnetic field in a vertical tube using two phase mixture model, Journal of Magnetism and Magnetic Materials 323 (2011) 1963–1972.

[36] S. Mirmasoumi, A. Behzadmehr, Numerical study of laminar mixed convection of a nanofluid in a horizontal tube using two-phase mixture model, Applied Thermal Engineering 28 (2008) 717–727

[37] Sh. Allahyari, A. Behzadmehr, S.M. Hosseini Sarvari, Conjugate heat transfer of laminar mixed convection of a nanofluid through a horizontal tube with circumferentially non-uniform heating, International Journal of Thermal Sciences 50 (2011) 1963-1972.

[38] M. Manninen, V. Taivassalo, S. Kallio, On the Mixture Model for Multiphase Flow, Technical Research Center of Finland, VTT Publications 288 (1996). 9–18.

[39] L. Schiller, A. Naumann, A drag coefficient correlation, Z. Ver. Deutsch. Ing. 77 (1935). 318–320.

[40] B.E. Launder, D.B. Spalding, Lectures in Mathematical Models of Turbulence, Academic Press, London, England, 1972.

[41] A.M. Hussein, K.V. Sharma, R.A. Bakar, K. Kadirgama, The Effect of Nanofluid Volume Concentration on Heat Transfer and Friction Factor inside a Horizontal Tube, Hindawi Publishing Corporation, Journal of Nanomaterials (2013) 859563.

[42] B.C. Pak, Y.I. Cho, Hydrodynamic and heat transfer study of dispersed fluids with submicron metallic oxide particles. Exp Heat Transfer 11(1998) 151–70.

[43] S.U.S. Choi, Z.G. Zhang, P. Keblinski, Nanofluids. Encyclopedia of Nanoscience and Nanotechnology 6 (2004) 757–773

[44] J. Buongiorno, Convective transport in nanofluids, ASME J of Heat Transfer 128 (2006) 240–250.

[45] C.H. Chon, K.D. Kihm, S.P. Lee, S.U.S. Choi, Empirical correlation finding the role of temperature and particle size for nanofluid (Al_2O_3) thermal conductivity enhancement, J. Phys. 82 (2005) 1–3.

[46] N. Masoumi, N. Sohrabi, A. Behzadmehr, A new model for calculating the effective viscosity of nanofluids, J. Phys. 42 (2009) 055501.

[47] K. Khanafer, K. Vafai, M. Lightstone, Buoyancy-driven heat transfer enhancement in a two-dimensional enclosure utilizing nanofluids, International Journal of Heat and Mass Transfer 46 (2003) 3639–3653.

[48] V. Gnielinski, New equations for heat and mass transfer in turbulent pipe and channel flow. International Chemical Engineering 16 (1976) 359-368.

[49] E.B. Haghighi, A.T. Utomo, M. Ghanbarpour, A.I.T. Zavareh, H. Poth, R. Khodabandeh, A. Pacek, B.E. Palm, Experimental study on convective heat transfer of nanofluids in turbulent flow: Methods of comparison of their performance, Experimental Thermal and Fluid Science 57 (2014) 378–387.

[50] S. Torii, Turbulent Heat Transfer Behavior of Nanofluid in a Circular Tube Heated under Constant Heat Flux, Hindawi Publishing Corporation Advances in Mechanical Engineering, 2 (2010) 917612.